The 2010 IEEE/RSJ International Conference on
Intelligent Robots and Systems
October 18-22, 2010, Taipei, Taiwan

Visual Segmentation of Lawn Grass for a Mobile Robotic Lawnmower

Alexander Schepelmann, Richard E. Hudson, Frank L. Merat, *IEEE Senior Member*, Roger D. Quinn, *IEEE Member*

***Abstract*—We investigate the existence of computationally inexpensive first and second order statistics that uniquely describe grass for application in an autonomous lawnmower. We then segment images based on these statistics to determine locations of driveable terrain in an image. Tight statistical clustering of illuminated grass versus artificial texture suggests that this method is sufficient for identifying driveable terrain for an autonomous lawnmower.**

I. Introduction

CWRU Cutter is an autonomous lawnmower developed at Case Western Reserve University for entry in the "Institute of Navigation (ION): Autonomous Lawnmower Competition." The robot serves as a proof-of-concept prototype that demonstrates it is possible to autonomously mow lawn and achieve the same quality of cut as a human operator. In previous years, CWRU Cutter placed 3rd and 1st in the ION competition by relying on LIDAR to sense obstacles. Though LIDAR is a robust sensor for autonomous robot applications, its price makes its inclusion in consumer versions of the robot prohibitively expensive. Computer vision, on the other hand, is able to extract similar useful information for a fraction of the cost of a LIDAR.

Mobile robots frequently rely on computer vision to differentiate between traversable terrain and obstacle locations [2][3]. This information is often based on the observed color of an object defined in the RGB model [1]. While RGB color can be a robust indicator of surfaces in scenes where light level is fairly constant and observed surface color is fairly uniform, its effectiveness drastically declines if an observed surface has significant color variation or is observed at multiple illumination levels as the mobile robot passes through areas occluded by shadows [11].

Hue has been shown to be a robust indicator of an objects' color in an applied environment [4][5][11][12]. This makes it a functional method of identifying an object's color in shaded areas. However, this method also fails to identify all of the traversable terrain in an image if a significant amount of color variation exists in the observed surface, as is the case with typical suburban lawns [15][16].

With increases in processing speed, visual texture is becoming an option for real-time identification of traversable terrain in incoming images. Since texture is a measure of underlying surface characteristics, it performs well in areas that have non-uniform lighting conditions [10][16]. However, there is no universal description of what constitutes a "texture". Texture identifiers are often based on computationally intensive, higher-order statistical calculations to classify an object's texture properties [7]. While these methods have been successfully and consistently used to quantify visual texture in images, their computation requirements limits their application for real-time operation in commercially available mobile robots that possess limited computational resources [8][9][5].

In this paper, we propose a small set of texture identifiers based on computationally inexpensive first and second order statistics to consistently identify grass-containing regions in an image and quantify the image statistics for our camera setup (described below). Previously, texture statistics of this order have been used to successfully differentiate between weeds and grass in robotic agricultural applications [16]. Four statistical measures were analyzed in horizontally oriented, vertically oriented, and directionally ambiguous grayscale and binary textures. These measures are mean grayscale neighborhood intensity, binary neighborhood variance, binary edge response area, and binary neighborhood centroid location (defined in Sect. III). Based upon clustering of the resulting texture statistics for illuminated grass and artificial obstacles, driveable terrain identification via surface texture seems to be a suitable method for application in an autonomous lawnmower. The clustering behavior of individual statistical measurements suggests that each statistic has a specific utility, which, when combined with other statistical measurements could provide improved performance for identifying grass in an image.

II. Data Collection

Image data were collected on a test plot containing a common grass mixture for typical North American suburban lawns at a local lawnmower manufacturer's testing facility. Test data were acquired using a camera elevated 0.75 meters at an angle of –45º to the horizontal. The camera was on a fixed mount on a collapsible dolly cart and mirrored the geometry of the CWRU Cutter autonomous lawnmower. The camera was an ImagingSource DFK21AF04 FireWire

Manuscript received March 10, 2010. This work was supported in part by MTD Products, Inc.

A. Schepelmann and R. D. Quinn are with the department of Mechanical and Aerospace Engineering, Case Western Reserve University, 10900 Euclid Ave, Cleveland, OH, USA 44106-7222 phone for A. Schepelmann: 216-392-9189; e-mail: axs287@case.edu, rdq@case.edu.

R. E. Hudson and F. L. Merat are with the department of Electrical Engineering and Computer Science, Case Western Reserve University, 10900 Euclid Ave, Cleveland, OH, USA 44106-7222 phone for R.E. Hudson: 216-704-6961; e-mail: reh2@case.edu, flm@po.cwru.edu.

camera with a Kowa LM4PBR 4.0mm F1.2 CS-Mount lens. Images were collected during a two-hour period in the mid-morning, to correspond to typical lighting conditions an autonomous lawnmower may experience in the field. Logged images included the following objects and conditions: 640x480 images of fully illuminated grass, as well as 50x50 image regions taken at 640x480 resolution of each of the following surfaces: shaded grass, flowerbed edging, flowers, blue jeans, fence, and a soccer ball. Statistical measurements were collected for a mixture of both illuminated and shaded obstacles to simulate common conditions an autonomous lawnmower may encounter [6].

III. TEXTURE EXTRACTION AND DESCRIPTORS

In this paper, we define "visual texture" as a collection of edges within an image region or "neighborhood." Within these neighborhoods, we examined four statistical measures of observed objects and texture image combinations: 1.) variance of horizontally and vertically oriented binary texture images, 2.) mean binary texture edge response area of horizontally and vertically oriented binary texture images, 3.) mean intensity of horizontally and vertically oriented grayscale texture images, and 4.) centroid location of directionally ambiguous binary texture images created by combining corresponding binary horizontal and vertical texture images within a neighborhood. A binary representation of grass-containing regions in the image, or "freespace," is generated from each statistic. This yields seven binary freespace representations.

Horizontal and vertical edge responses were extracted by convolving an unblurred, grayscale image (Fig. 1a) with a horizontal (*Gx*) and vertical (*Gy*) Prewitt convolution kernel, respectively, given by

$$Gx = \begin{bmatrix} -1 & 0 & +1 \\ -1 & 0 & +1 \\ -1 & 0 & +1 \end{bmatrix} \quad (1)$$

and

$$Gy = \begin{bmatrix} -1 & -1 & -1 \\ 0 & 0 & 0 \\ +1 & +1 & +1 \end{bmatrix} \quad (2)$$

The convolution operation computes the edge strength based on grayscale intensity values of a pixel and its eight adjacent neighbors and plots the magnitude of the edge strength in the center pixel. The 2D spatial convolution operation is given by

$$E(x,y) = \sum_{j=0}^{J-1}\sum_{k=0}^{K-1} G(j,k)I(x-j,y-k) \quad (3)$$

where *E(x,y)* is the computed edge strength of a pixel located in the center of a 3x3 neighborhood located at (*x,y*) in the image, $j \rightarrow J\text{-}1$ and $k \rightarrow K\text{-}1$ are the indices of the convolution kernel *G*, and *I(a,b)* is the intensity value of a pixel located at the input coordinate pair (*a,b*). Convolving the image with *Gx* and *Gy* generates two new images that indicate edge response for the given filter. We refer to the resulting images as "horizontal-" and "vertical texture images," respectively (Fig. 1b).

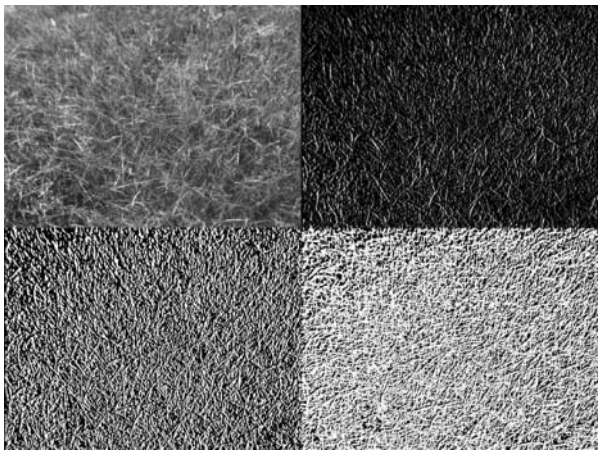

Fig. 1. Clock-wise from top-left: a. Grayscale image of grass, b. Grayscale horizontal texture image of Fig. 1 a., c. Binary horizontal texture image of Fig. 1 a., d. Directionally ambiguous binary texture image of Fig. 1 a.

From the resulting oriented grayscale texture images, horizontal and vertical binary texture images were created by discarding edge strengths below an empirically determined threshold of 21 and setting corresponding pixel locations of edge strength above the threshold in a binary image equal to 1. Pixel groupings with an area of 1 in the binary images were removed (Fig. 1c).

Summing corresponding horizontal and vertical binary texture images yielded the directionally ambiguous binary texture image corresponding to the input image (Fig. 1d).

We examined statistics for four square neighborhoods ranging from 11x11 to 41x41 pixels in increments of 10 pixels.

The variance for each neighborhood, *Var(R)*, of the horizontal and vertical binary texture images was computed by

$$Var(R) = \left(\sum X - \overline{X}\right) \Big/ (n-1) \quad (4)$$

where *X* is the binary value of the current pixel, $\overline{X}$ is the mean value of the pixels within the square neighborhood, and *n* is the area of the neighborhood, given by the total number of pixels within the neighborhood. Since we are computing the variance of a binary neighborhood, this reduces to a polynomial in one dimension

$$Var(R) = \left(w - \left(w^2 \Big/ n\right)\right) \Big/ (n-1) \quad (4)$$

where *w* is the number of pixels in the neighborhood above the binary threshold.

The mean grayscale intensity value of a neighborhood was computed by summing all pixel values of the generated grayscale texture images and dividing by the total number of pixels within the neighborhood.

The binary area and centroid locations of the pixel neighborhoods were calculated as

$$M_{ij} = \sum_x \sum_y x^i y^j I(x,y) \quad (5)$$

where the calculated moment M_{ij} is given by the summation over the x and y dimensions of the pixel neighborhood, and i and j correspond to the index of the calculated moment. The binary area is given by M_{00}, and the horizontal and vertical centroid locations within the neighborhood, $\bar{x}$ and $\bar{y}$, respectively, of the directionally ambiguous texture image are given by

$$\bar{x} = M_{10} / M_{00} \quad (6)$$

and

$$\bar{y} = M_{01} / M_{00} . \quad (7)$$

After determining the statistical values for grass in the set of training images, non-overlapping binary segmentation was applied to neighborhoods of images based on these measurements. Non-overlapping neighborhoods were used to decrease the runtime of the algorithm. If the measured statistic of the neighborhood fell within three standard deviations of the observed statistical measurements from training, that neighborhood was marked as grass. Conversely, if the neighborhood measurements fell outside this range, the neighborhood was marked as containing an obstacle. The binary representations of freespace in the camera frame can later be post-processed and combined across the images for corresponding neighborhoods to create an improved texture-based representation of traversable terrain in the image.

IV. Quantification of Texture Descriptors

After calculating the statistics for the texture images, we computed the mean and standard deviation (σ) of the statistics for each surface type at each neighborhood size to observe groupings in the measurements. Table 1 displays calculated statistics of sample neighborhoods for a neighborhood size of 31. We then plot like statistics of each surface type at different neighborhood sizes in the same graph to visually display groupings. The following data was plotted for each neighborhood size: Mean neighborhood intensity of grayscale horizontal (hTx) vs. vertical (vTx) texture images for corresponding neighborhoods ($\bar{I}$), variance of binary horizontal vs. vertical texture images for corresponding neighborhoods ($\overline{Var(R)}$), mean edge response area of binary horizontal vs. vertical texture images for corresponding neighborhoods ($\bar{A}$), and local horizontal and vertical centroid location for corresponding neighborhoods of directionally ambiguous binary texture images ($\bar{x}, \bar{y}$).

V. Results & Discussion

The goal of vision processing in the autonomous lawnmower is to identify driveable terrain around the robot by identifying grass. Observed image regions that do not match the measured grass statistics are marked as "obstacle containing regions." This creates a binary freespace map around the robot for every camera frame, which is abstracted into range images via the method presented in [5]. Since we do not attempt to distinguish between different types of obstacles, we plot all non-grass data points in the following plots with the same color (with the exception of flowers) for visualization purposes (Figs. 2-7). We will refer to the visual texture of fence, flowerbed edging, blue jeans, and soccer ball as "artificial texture," as these objects are manmade. Similarly, we will refer to these obstacles as "artificial." In all plots, surface textures correspond to the following point color: green – illuminated grass, yellow – shaded grass, magenta – flowers, red – artificial obstacles.

For the binary statistics, we observed distinct, compact clustering of illuminated grass for all neighborhood sizes (Figs. 3-5). Mean values of the clusters for oriented texture measurements are close to the diagonal of the plots, indicating no strong directionality for either the horizontal or vertical texture images. This indicates that both horizontal and vertical texture images identify illuminated grass equally well, and that filter orientation is not a determining factor in being able to identify grass based on observed statistics.

Across all statistics, we observed that the distribution of illuminated grass data points compacted as the neighborhood size increased (Fig. 2, 6). This results from the fact that a larger neighborhood is less sensitive to variations in individual pixels, thereby decreasing the overall standard

TABLE I
NEIGHBORHOOD STATISTICS FOR NEIGHBORHOOD SIZE OF 31

Measurement / Surface Type	Illuminated Grass	Shaded Grass	Flowerbed Edging	Flowers	Jeans	Soccer Ball
$\bar{I}$ (hTx,,vTx)	(-0.922, -10.169)	(-.027, -4.685)	(1.408, -5.644)	(-4.334, -13.333)	(0.251, -7.427)	(-4.739, -17.794)
$\sigma(\bar{I})$ (hTx, vTx)	(5.053, 3.288)	(1.637, 1.225)	(5.749, 6.764)	(17.224, 12.480)	(8.535, 4.655)	(15.448, 12.688)
$\overline{Var(R)}$ (hTx, vTx)	(0.231, 0.225)	(0.164, 0.144)	(0.088, 0.124)	(0.172, 0.191)	(0.090, 0.065)	(0.068, 0.098)
$\sigma(\overline{Var(R)})$ (hTx, vTx)	(0.010, 0.014)	(0.039, 0.045)	(0.075, 0.066)	(0.0519, 0.0419)	(0.053, 0.067)	(0.056, 0.062)
$\bar{A}$ (hTx, vTx)	(350.590, 332.810)	(203.90, 172.80)	(103.80, 150.70)	(221.30, 261.20)	(101.40, 76.10)	(74.90, 112.40)
$\sigma(\bar{A})$ (hTx, vTx)	(31.976, 39.559)	(59.056, 57.965)	(94.373, 92.161)	(76.288, 83.751)	(64.547, 87.778)	(65.829, 73.552)
($\bar{x}$, $\bar{y}$)	(15.368, 15.015)	(15.415, 14.570)	(7.465, 13.008)	(16.691, 15.120)	(15.527, 13.126)	(18.407, 14.952)
$\sigma(\bar{x}, \bar{y})$	(0.606, 0.599)	(0.951, 0.722)	(2.564, 1.067)	(2.469, 2.000)	(2.473, 6.364)	(6.152, 5.322)

deviation of plotted points.

Variance measurements from oriented binary texture images exhibited distinct clustering behavior from artificial obstacles (Fig. 3). The color uniformity of artificial obstacles resulted in data points near the plot origin, such as a fence post. Images of an artificial obstacle border exhibit strong unidirectional texture response. Artificial object texture was distributed uniformly between the origin and approximately (0.20, 0.20) for all resolutions. Conversely, illuminated grass had significantly different, tightly clustered variation for both horizontal and vertical binary texture images. Observed variance of illuminated grass was the same for horizontal and vertical binary texture and did not change as neighborhood size increased, being centered at approximately (0.25, 0.25). Noticeable separation between illuminated grass and artificial obstacles again occurred at neighborhood sizes of 31x31 or greater.

Mean binary edge response area exhibited separation at all neighborhood sizes. As neighborhood size increased, the edge response area of illuminated grass increased as well, whereas areas of artificial obstacles remained constant due to low edge response. Distinguishable separation of artificial obstacles and illuminated grass areas was again observed for neighborhood sizes greater than or equal to 31x31 (Fig. 4).

For all neighborhood sizes, tight clustering of neighborhood centroid location was observed for illuminated grass, whereas artificial obstacles did not exhibit tight clustering (Fig. 5).

All statistics contained overlap between the flower obstacle and shaded grass. Flower textures were generally distinct from artificial obstacle textures, being either located in a different region in the graph or exhibiting a tighter clustering than the artificial textures. An overlap consistently existed for all statistical measurements between flowers and shaded grass. Both of these behaviors are attributed to the same phenomenon. While illuminated grass was the most "rough" texture in observed images, because it

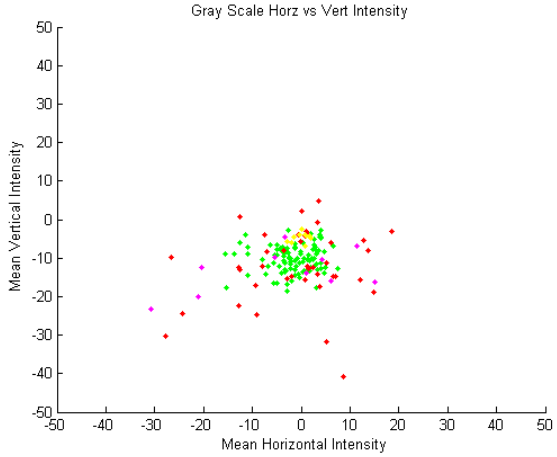

Fig. 2. Horizontal vs. vertical grayscale texture intensity for observed surfaces at 31x31 neighborhood size. While illuminated (green) and shaded (yellow) grass clusters overlap, artificial obstacles (red) and flowers (magenta) are uniformly distributed at similar intensity values.

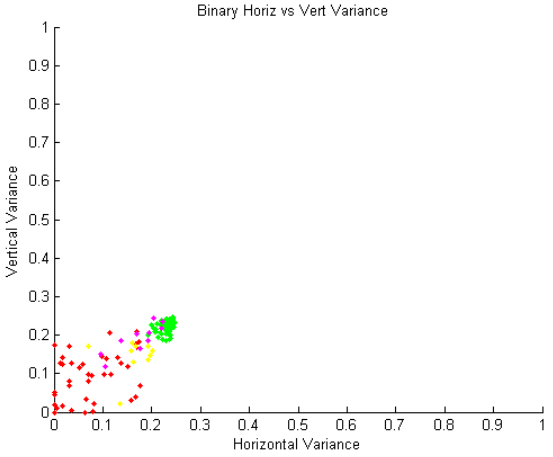

Fig. 3. Horizontal vs. vertical binary texture variances for observed surfaces at 31x31 neighborhood size with an edge threshold value of 21. Illuminated grass (green) clusters, whereas artificial obstacles (red) and flowers (magenta) are distributed at a lower variance value than illuminated grass. Shaded grass (yellow) is not clustered.

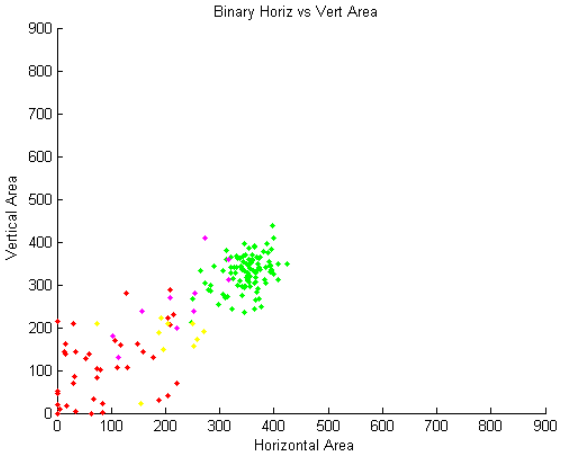

Fig. 4. Horizontal vs. vertical binary edge response area for observed surfaces at 31x31 neighborhood size with an edge threshold value of 21. Illuminated grass (green) clusters, whereas artificial obstacles (red) and flowers (magenta) are distributed at lower area values than illuminated grass. Shaded grass (yellow) is not clustered.

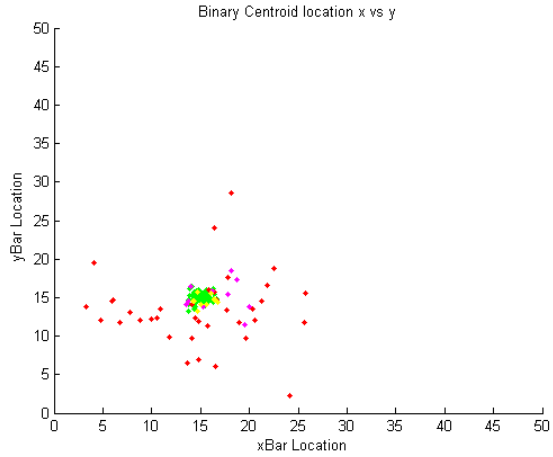

Fig. 5. Horizontal vs. vertical binary texture neighborhood centroid location for observed surfaces at 31x31 neighborhood size with an edge threshold value of 21. Illuminated grass (green) clusters, whereas artificial obstacles (red) are distributed at a lower variance value. Flowers (magenta) exhibit clustering and overlap somewhat with illuminated grass. Shaded grass (yellow) clusters in the same area as illuminated grass.

TABLE II
NUMBER OF CORRECTLY IDENTIFIED TEXTURE REGIONS

Measurement	$\overline{Var(R)}_{hTx}$	$\overline{Var(R)}_{vTx}$	$\overline{A}_{hTx}$	$\overline{A}_{vTx}$	$(\overline{x}, \overline{y})$	$\overline{I}_{hTx}$	$\overline{I}_{vTx}$
Grass	40	40	38	38	40	38	14
Shadow	36	36	36	36	39	40	8
Obstacles	37	31	35	35	28	10	33
Flowers	11	5	9	9	21	14	27

contained many edges per neighborhood, artificial obstacles were the "smoothest", having little color variation, which caused a low edge response. While flowers were less rough than illuminated grass, they were nearly equally as smooth as shaded grass in grayscale and binary textures. Performance of binary texture distinction and clustering of shaded grass did not change significantly as the edge threshold was lowered (Fig. 7).

Based on these results, individual statistics have the following utility: Binary directional variance, directional binary edge response area, and directionally ambiguous centroid location are useful for determining areas of illuminated grass in an image due to their compact clustering compared to artificial obstacles. Mean grayscale intensity did not exhibit useful behavior for the calculated statistics.

The regional runtime of this method as implemented in MATLAB was approximately 15 kHz for 21x21 pixel neighborhoods. Other general-purpose texture analysis methods can be more computationally expensive. For example, the method proposed in [7] operated at approximately 30 Hz per region on similar hardware (Windows XP based PC with a 2.00 GHz Core 2 Duo processor and 2 GB of RAM).

Grass identification via these statistics was tested on 40 randomly selected samples of 31x31 neighborhoods containing: illuminated grass, shaded grass, artificial obstacles, and flowers. These results are tabulated in Table 2, which lists the number of correctly identified texture regions. Illuminated grass was correctly identified with at least 95% accuracy for all texture measurements except mean vertical grayscale intensity. Shaded grass was identified with at least 90% accuracy for all texture measurements except the mean vertical grayscale intensity. Binary horizontal variance and binary horizontal and vertical area identified obstacles correctly with at least 87.5% accuracy. Flowers were poorly identified. We believe that this may be due to texture similarity between the grass and flowers.

Segmentation based on each measured statistic of illuminated grass for 31x31 neighborhoods was performed for 300 regions in 640x480 images. These images emulated typical scenes that a lawnmower may encounter in a suburban environment. Sample segmentation results of the horizontal binary variance and binary centroid locations are displayed in Figs. 9-10. Each statistic successfully managed to differentiate between artificial obstacles and grass. While segmentation successfully recognized areas with multiple flower buds, it failed to recognize flower areas with a high amount of stems and/or leaves. Failure to identify all flower regions is again attributed to the roughness of the flower obstacle, unlike the flowerbed edging whose texture is significantly smoother than either the illuminated or shaded grass.

The focus of future research will be to eliminate false positives in the resulting binary freespace representations. This could be done by post-processing outputs individually by removing freestanding neighborhoods or neighborhood groupings less than an area corresponding to the smallest

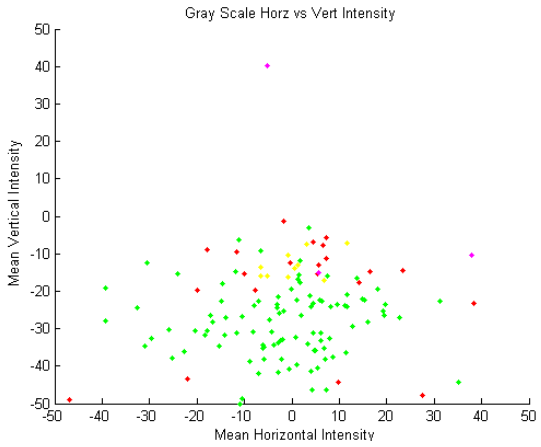

Fig. 6. Horizontal vs. vertical grayscale texture intensity for observed surfaces at 11x11 neighborhood size. Distinct clustering between illuminated grass (green), shaded grass (yellow), artificial obstacles (red), and flowers (magenta) was not observed. This phenomenon was consistent for binary variance measured statistics as well.

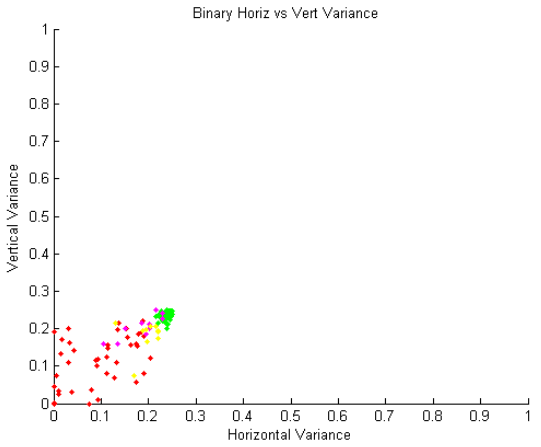

Fig. 7. Horizontal vs. vertical binary variance for observed surfaces at 31x31 neighborhood size with an edge threshold value of 10. Compared to Fig. 3, location of clustering did not significantly change as the edge threshold value was lowered.

obstacle the lawnmower is likely to encounter. Freespace representations could then be combined across generated outputs by comparing how many statistics agree that the current neighborhood is grass and creating a probability map of driveable terrain in the image.

Additionally, abstracted binary freespace representations into range images via the method presented in [5] can be merged using existing methods such as those presented in [14] for a best estimate of freespace around the robot.

VI. Conclusions

We investigated grayscale and binary texture extraction via image convolution and quantified the observed textures via first and second order statistics in an attempt to identify grass for navigational use by an autonomous lawnmower. We show that illuminated grass has a distinct texture compared to artificial obstacles based on these statistics. To demonstrate this, we classified test images of illuminated grass, shaded grass, artificial obstacles, and flowers based on these statistics. This created texture-based binary freespace representations of grass in an image. Our results indicate that it is possible to identify grass from artificial obstacles, which future work will use for obstacle avoidance purposes in an autonomous lawnmower. Since the analyzed images contained well-illuminated grass and heavy shadows, we believe that these descriptors are able to identify grass with a high degree of accuracy at intermediate lighting conditions as well. While each statistic was not able to identify every neighborhood correctly by itself, we posit that recognition performance could be improved through a combination of these results by creating a probability map of driveable terrain or through sensor fusion techniques.

References

[1] S. Thrun *et al.*, "Stanley: The robot that won the DARPA grand challenge: Research articles," J. Robot. Syst, vol. 23, no. 9, pp. 661–692, 2006.

[2] P. Bellutta, R. Manduchi, L. Matthies, and K. Owens, "Terrain Perception for Demo III", IEEE Intelligent Vehicle Symposium, Dearborn, USA, October 2000.

[3] G.N. De Souza, A.C. Kak, "Vision for mobile robot navigation: A survey," IEEE Transactions on Pattern Analysis and Machine Intelligence, vol. 24, no. 2, pp. 237–267, 2002.

[4] J. G. Liu, J. M. Moore "Hue image RGB colour composition. A simple technique to suppress shadow and enhance spectral signature," International Journal of Remote Sensing, vol. 11, no. 8, pp. 1521 – 1530, 1990.

[5] A. Schepelmann, H. H. Snow, B. E. Hughes, F. L. Merat, R. D. Quinn, and J. M. Green, "Vision-Based Obstacle Detection and Avoidance for the CWRU Cutter Autonomous Lawnmower," IEEE International Conference on Technologies for Practical Robot Applications, Boston, USA, November 2009, pp. 218-232.

[6] *The Sixth Annual Robotic Lawnmower Competition Rulebook*. Dayton, Ohio: Institute of Navigation, 2009. [Online]. Available: http://www.ion.org/satdiv/alc/rules2009.pdf. [Accessed: July 24, 2009].

[7] Y. Karklin and M. S. Lewicki. "Learning higher-order structures in natural images." Network: Computation in Neural Systems, vol. 14, pp. 483-499, 2003.

[8] M. Montemerlo, S. Thrun, H. Dahlkamp, D. Stavens, and S. Strohband, "Winning the DARPA Grand Challenge with an AI robot," In Proc. of the AAAI National Conference on Artificial Intelligence, pp. 17-20, 2006.

[9] J. Bohren, *et al.*, "Little Ben: The Ben Franklin Racing Team's Entry in the 2007 DARPA Urban Challenge, Journal of Field Robotics, vol. 25, no. 9, pp. 598-614, 2008.

[10] A. Broggi, C. Caraffi, P. P. Porta, and P. Zani, "The Single Frame Stereo Vision System for Reliable Obstacle Detection used during the 2005 DARPA Grand Challenge on TerraMax," Proc. of the IEEE ITSC 2006, Sept 17-20,2006, pp. 745-752.

[11] M. Zaheer Aziz , B. Mertsching , M. Salah E. N. Shafik , and R. Stemmer, "Evaluation of Visual Attention Models for Robots," Proc. of the Fourth IEEE International Conference on Computer Vision Systems, vol. 20, January, 2006.

[12] J. Hemming and T. Rath, "Computer-Vision-Based Weed Identification Under Field Conditions Using Controlled Lighting," J. Agricultural Engineering Research, vol. 78, no. 3, pp. 233-243.

[13] I. Philipp and T. Rath, "Improving Plant Discrimination in Image Processing by Use of Different Colour Space Transformations," Computers and Electronics in Agriculture, 35, pp. 1-15, 2002.

[14] B. Zafarifar and P. H. N. de With, "Grass Field Detection for TV Picture Quality Enhancement," IEEE International Conference on Consumer Electronics, Las Vega, USA, January 2008, pp. 329-330.

[15] D. E. Karcher and M. D. Richardson, "Quantifying Turfgrass Color Using Digital Image Analysis," Crop Science, vol. 43, no. 3, pp. 943-952, 2003.

[16] U. Watchareeruetai, *et al.,*"Computer Vision Based methods for Detecting Weeds in Lawns," Machine Vision and Applications, vol. 17, pp. 287-296, 2006.

Fig. 8. Illuminated grass, shaded grass, artificial texture flowerbed edging, and natural texture flower obstacles.

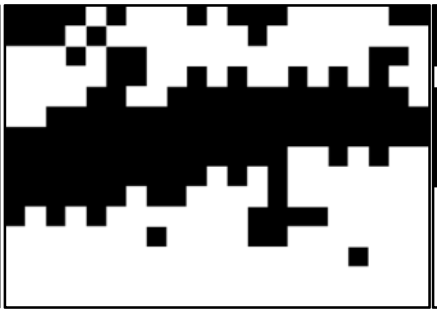

Fig. 9. Segmentation results of Fig. 8 based on horizontal binary variance statistics for 31x31 neighborhoods. This statistic recognizes the majority of illuminated and shaded grass as driveable terrain (white regions), while marking the flowerbed edging and some flower buds at the top of the image as obstacle containing (black).

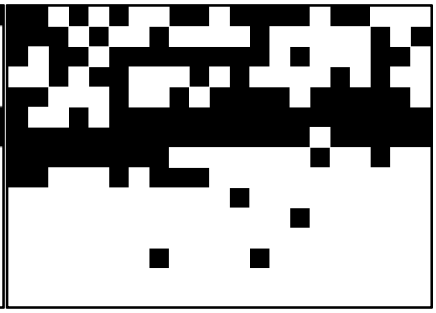

Fig. 10. Segmentation results of Fig. 8 based on binary centroid location of illuminated grass for 31x31 neighborhoods. This statistic also recognizes grass as driveable terrain (white regions), while marking the flowerbed edging and many flower buds as obstacles (black).